

Estimating lake–atmosphere CO₂ exchange

Dean E. Anderson, Robert G. Striegl, David I. Stannard, and Catherine M. Michmerhuizen

U.S. Geological Survey, Box 25046, MS 413, Denver, Colorado 80225-0046

Ted A. McConnaughey

Biosphere 2 Research, P.O. Box 689, Oracle, Arizona

James W. LaBaugh

U.S. Geological Survey, 12201 Sunrise Valley Drive, Reston, Virginia

Abstract

Lake–atmosphere CO₂ flux was directly measured above a small, woodland lake using the eddy covariance technique and compared with fluxes deduced from changes in measured lake-water CO₂ storage and with flux predictions from boundary-layer and surface-renewal models. Over a 3-yr period, lake–atmosphere exchanges of CO₂ were measured over 5 weeks in spring, summer, and fall. Observed springtime CO₂ efflux was large (2.3–2.7 μmol m⁻² s⁻¹) immediately after lake-thaw. That efflux decreased exponentially with time to less than 0.2 μmol m⁻² s⁻¹ within 2 weeks. Substantial interannual variability was found in the magnitudes of springtime efflux, surface water CO₂ concentrations, lake CO₂ storage, and meteorological conditions. Summertime measurements show a weak diurnal trend with a small average downward flux (–0.17 μmol m⁻² s⁻¹) to the lake’s surface, while late fall flux was trendless and smaller (–0.0021 μmol m⁻² s⁻¹). Large springtime efflux afforded an opportunity to make direct measurement of lake–atmosphere fluxes well above the detection limits of eddy covariance instruments, facilitating the testing of different gas flux methodologies and air–water gas-transfer models. Although there was an overall agreement in fluxes determined by eddy covariance and those calculated from lake-water storage change in CO₂, agreement was inconsistent between eddy covariance flux measurements and fluxes predicted by boundary-layer and surface-renewal models. Comparison of measured and modeled transfer velocities for CO₂, along with measured and modeled cumulative CO₂ flux, indicates that in most instances the surface-renewal model underpredicts actual flux. Greater underestimates were found with comparisons involving homogeneous boundary-layer models. No physical mechanism responsible for the inconsistencies was identified by analyzing coincidentally measured environmental variables.

Gaseous flux between large natural water bodies and the atmosphere is a subject of considerable interest (Liss and Slater 1974; Liss 1983; Kraus and Businger 1994) and one that is critical for determining the global carbon balance (Keeling et al. 1989). Lakes are a small but globally significant source of carbon to the atmosphere, contributing about 0.14×10^{15} g yr⁻¹ (based on model estimates of Kling et al. 1991 and Cole et al. 1994). Air–water gas exchange may be estimated by a variety of indirect means, including analysis of certain geochemical cycles, tracer methods, and enclosures (MacIntyre et al. 1995). From these data, simple equations involving a transfer velocity and the air–water concen-

tration gradient of gas may be calibrated to estimate gas flux. CO₂ flux (F_c) may be estimated by multiplying the calculated transfer velocity derived from a homogeneous boundary-layer or surface-renewal model (Jahne et al. 1987; MacIntyre et al. 1995) by routine measurements of the air–water [CO₂] difference (brackets indicate concentration). Slight modifications to this approach are used to estimate global ocean–atmosphere F_c (Thomas et al. 1988; Van Scoy et al. 1995).

In contrast to these methods, eddy covariance offers an opportunity to directly measure trace gas fluxes without affecting natural gas transfer between water and air. Mass flux of CO₂ above a surface is obtained by measuring the mean covariance of the deviations from the mean in vertical velocity (w′) and the mixing ratio of CO₂ (C′). F_c is computed as

$$F_c = \overline{w'C'} \quad (1)$$

where $w' = w - \bar{w}$, w is an instantaneous value, and \bar{w} is the mean. (C′ may be similarly written.) The mixing ratio is $C = \rho_c/\rho_a$, where ρ_c is the absolute density of CO₂ and ρ_a is dry-air density. Ordinarily, ρ_c is measured instead of C, resulting in a more complex calculation of F_c (see Webb et al. 1980 for details).

Although eddy covariance measurement theory is rather simple, its application in the measurement of typically small (relative to terrestrial vegetation) F_c fluxes over oceans (Jones and Smith 1977; Wesely et al. 1982; Smith and Jones

Acknowledgments

We are grateful to E. P. Weeks (U.S. Geological Survey, Denver) for his very helpful support, discussions, and review of this manuscript, which led to substantial improvements in its content. We also express our thanks to Renee Parkhurst for assistance in data retrieval, the late Dennis Merk for maintaining equipment and infrastructure at the lake, Dr. Shashi Verma for an equipment loan, and to Drs. Marvin Wesley, Shashi Verma, and two anonymous journal reviewers for their helpful reviews of this manuscript. This work was funded by the U.S.G.S. Global Change Hydrology Program.

Any use of trade, product, or firm names in this document is for descriptive purposes only and does not imply endorsement by the U.S. Geological Survey.

1985) has generated considerable controversy (O'Brian 1986), particularly because flux estimates from it were found to be substantially larger than those determined from isotopic and tracer methods (Broecker et al. 1986). A critique of methods and measurements solicited by O'Brian (1986) identified several possibilities for the differences, although the issue largely remains unresolved. The eddy covariance measurements were made in near-shore environments, which are characteristically highly variable in temperature and surface-water CO₂ concentrations, [CO_{2, aq}]. Due to local spatial and temporal heterogeneity of [CO_{2, aq}] within the flux footprint (*see* Schuepp et al. 1990 and Horst and Weil 1992 for a definition of this term) of eddy covariance measurements, it becomes very difficult to accurately relate fluxes to concentration differences driving them (Crawford et al. 1993). Additionally, there is the potential for enhanced fluxes near breaking waves (Wallace and Wirrick 1992), which more frequently occur in coastal areas.

Regarding air–water gas exchanges over freshwater lakes, we know of only two other studies of F_c. Wesely et al. (1982) made direct measurements of F_c using eddy covariance instruments during a 1-d period above Lake Michigan; they found general agreement with transfer velocities derived from radon tracer experiments. Denmead and Freney (1992), working over a flooded agricultural field, made comprehensive measurements of air and surface water [CO₂]. They estimated F_c using the aerodynamic-profile approach, an indirect micrometeorological method. Derived transfer velocities were found to agree with those calculated from a homogeneous boundary-layer model (Deacon 1977). During the experiment, [CO_{2, aq}] rose from undersaturated to supersaturated levels with respect to the atmosphere. In summary, we find that the freshwater data set is too small to determine whether there are systematic differences between measured and modeled fluxes or transfer velocities.

This paper focuses on estimating air–water exchange of CO₂ at a small groundwater-dominated lake. The lack of surface-water interactions of the chosen lake facilitates comparison of fluxes independently derived from eddy covariance and a lake-water CO₂ storage change method. It also simplifies the comparison of fluxes and transfer velocities derived from measurements with those from model estimates. Characteristics of lake–atmosphere exchange of CO₂ in different seasons is also examined.

Theoretical background

Current theory of gaseous transport between the atmosphere and water bodies conceptually involves a series of boundary-layers comprising both fluids (*see* Denmead and Freney 1992; MacIntyre et al. 1995). In the atmospheric surface layer over a lake, turbulent motions are principally responsible for transporting gas between the free atmosphere and the vicinity of the lake surface. Between the turbulent air and the surface lies a viscous or quasilaminar sublayer (approximately 1 mm thick) where molecular diffusion dominates gas transport. Immediately below the air–water interface is the viscous sublayer of water, also referred to as a water film or skin (on the order of tens of microns thick). It

is analogous to the viscous sublayer in air and typically contains sharp gradients in gas concentration and temperature. Below the aqueous viscous sublayer is the well-mixed bulk water column.

Dynamic boundary-layer theories consider that the thickness of the viscous sublayer changes as a function of wind speed and temperature (Deacon 1977). In contrast to boundary-layer theory, surface-renewal theory (Danckwerts 1951) contends that the aqueous, viscous sublayer is inhomogeneous. Conceptually, with the onset of instability due to thermal or density-driven convection, or with the onset of capillary waves whereby the water's surface area expands and contracts, the viscous sublayer is broken into patches so that a portion of the original skin layer is replaced by randomly distributed bulk water parcels. Skin patches in the surface-renewal model have a finite lifetime and size, typically defined by a probability density function (Rao et al. 1971).

In both boundary-layer and surface-renewal models, F_c is driven by a concentration difference (units of density) between the bulk water (C_w) and well-mixed atmosphere (C_a); it is governed by the bulk transfer velocity (V_B):

$$F_c = V_B \left(\frac{C_w}{S} - C_a \right). \quad (2)$$

Dimensionless solubility, S, is defined by the ratio of the equilibrium concentration of dissolved gas in water to that in air. S typically ranges between 0.7 and 0.8, varying with temperature ($S \propto T^{-7.5}$) and the physical chemistry of gas–water interactions (Deacon 1977; Denmead and Freney 1992).

For homogeneous boundary layers, V_B is closely approximated (Deacon 1977, 1981) by this equation:

$$V_B = \frac{\alpha S u_{*w}}{Sc_t^{1/3} Sc^\beta} \quad \text{for } Sc > 200, \quad (3)$$

where α and β are constants and the friction velocity of the water's surface (u_{*w}) is equal to the friction velocity in air (u_*) times the square root of the ratio of fluid densities (air and water). The Schmidt number (Sc) is the ratio of kinematic viscosity of a gas (1.6 mm² s⁻¹ at 5°C) to its diffusivity in water (1.1 mm² s⁻¹ at 5°C), while the turbulent Schmidt number (Sc_t) is the ratio of the turbulent transfer coefficient for momentum to that of the diffusing gas in air. Thus, both Sc and Sc_t are functions of skin (surface) temperature. Sc (=1,396 at 5°C, other values tabulated in MacIntyre et al. 1995) varies about 6% per degree Celsius near 5°C. The value of Sc_t is not well resolved, ranging from 0.7 to 1.0 (Deacon 1981). Deacon's (1977) smooth-surface formula (stagnant boundary layer) sets $\alpha = 0.082$ and $\beta = 2/3$. With gravity waves, surface renewal enhances flux by about two to three times that found through a stagnant boundary layer. To match flux under these conditions, Deacon (1981), Wesely et al. (1982), and Csanady (1990) determined that $\beta = 1/2$.

Because of the sensitivity of V_B to temperature (through Sc), skin temperature must be accurately estimated. Skin temperature may be a few degrees less than bulk water temperature because of radiative cooling and heat loss (latent and sensible). Conversely, radiative loading during the day

and sensible heat advection may warm the skin above the bulk water temperature. Although several surface-renewal formulations of V_B exist, we focused on that of Soloviev and Schlusel (1994 and 1996), which was derived for a wide range of wind and surface wave conditions during which mechanically and thermally induced renewal events occur. Building upon previous renewal model work and field studies, the Soloviev and Schlusel model incorporates surface heat flux and friction velocity to determine skin temperatures, which regulate thermal and gaseous diffusion through the skin layer. Surface-renewal events that may take place during calm conditions due to convection immediately below the surface were parameterized after Kudryavtsev et al. (1985). The surface Richardson number (Rf_o) was used to determine the transition from free to forced convection:

$$Rf_o = -\frac{\epsilon g \nu H_{wo}}{u_{*w}^4 \rho_w c_{pw}}, \quad (4)$$

where g is gravitational acceleration, ϵ is the thermal expansion coefficient of water, H_{wo} is the total surface heat (sensible, latent, and radiant) flux, c_{pw} is the specific heat of water, and subscript o indicates the surface. Skin temperature depression, or the difference between skin and bulk water temperatures, is given by Eq. 5:

$$\begin{aligned} \Delta T &= T_{*w} \Lambda_o Pr^{1/2} F(Rf_o, Ke) \\ &\approx T_{*w} \Lambda_o Pr^{1/2} \left[1 + \frac{Rf_o}{Rf_{cr}} \right]^{1/4} \left[1 + \frac{Ke}{Ke_{cr}} \right]^{1/2}, \end{aligned} \quad (5)$$

where T_{*w} is the characteristic surface temperature and Pr is the Prandtl number (ratio of water's molecular viscosity to its thermal diffusivity). Referencing cool-skin data gathered by others, Soloviev and Schlusel (1994) quantified constants Λ_o ($=13.3$) and the critical Richardson number, Rf_{cr} ($= -1.5 \times 10^{-4}$). Enhanced heat (and gas) transfer occurring after the transition from waves described as rollers to long-wave breakers is controlled by the Keugelan number ($Ke = u_{*w}^3/g\nu_w$) having the critical value $Ke_{cr} = 0.18$. The left side of Eq. 5 corresponds to eq. 21 in Soloviev and Schlusel (1994), while the right is a truncated version of that on the left, corresponding to Soloviev and Schlusel (1994) eq. 25. Gas transfer through the skin is given by Eq. 6:

$$\begin{aligned} V_B &= Au_{*w} [\Lambda_o Sc^{1/2} F(Rf_o, Ke)]^{-1} \\ &\approx Au_{*w} \left[1 + \frac{Rf_o}{Rf_{cr}} \right]^{1/4} \left[\Lambda_o Sc^{1/2} \left(1 + \frac{Ke}{Ke_{cr}} \right)^{1/2} \right]^{-1}, \end{aligned} \quad (6)$$

where calibration factor A ($=1.85$) is derived from Peng et al.'s (1979) radon tracer results. Note that this model does not attempt to account for regulation of flux by surface chemistry nor enhanced transfer caused by spray from higher wind speeds and breaking waves. Recently, Szeri (1997) has quantified the flux enhancement caused by deformation of the gas concentration fields in the presence of capillary waves. This convection-enhancement of flux is not included in Eq. 6; it requires knowledge of the distribution and slope profile of capillary waves in the ensemble wavefield.

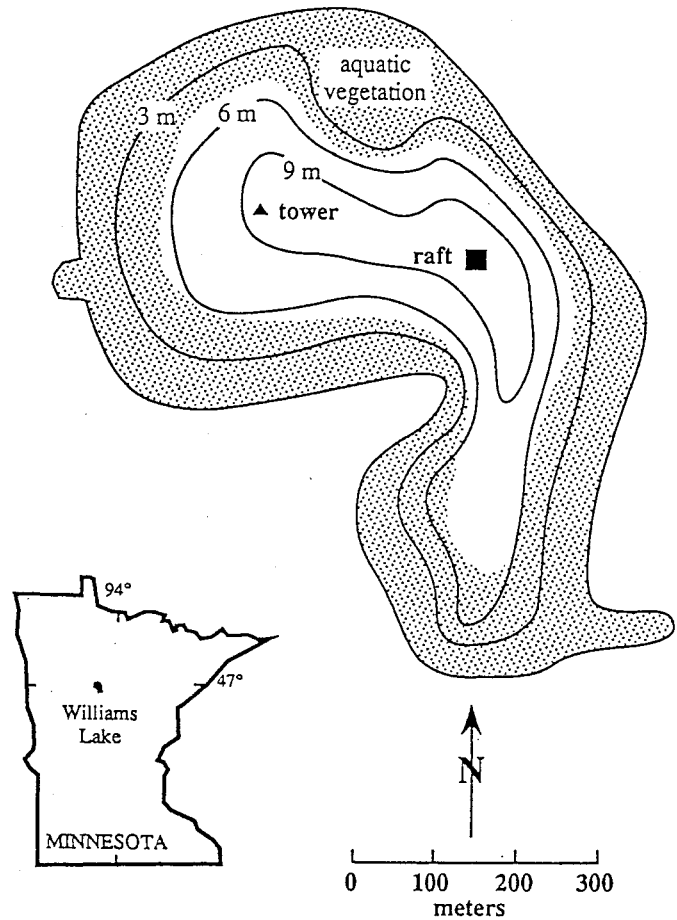


Fig. 1. Location and site map of Williams Lake showing positions of eddy covariance tower and auxiliary measurement raft.

Methods

Site—All measurements were performed at Williams Lake, Minnesota ($46^{\circ}57'N$, $94^{\circ}40'W$, 422 m elevation), the location of extensive previous and ongoing hydrologic and limnological investigations (Winter 1997). The lake lies in a mixed hardwood-conifer woodland and has no surface water inlets or outlets. The lake's surface area of 37.09 ha is ellipsoidal (900-m major axis running northwest-southeast, 550-m minor axis), punctuated by a low peninsula protruding in the southwestern quarter of the lake, as depicted in Fig. 1. Lake volume is 2×10^6 m³ and average depth is 5.2 m (9.3 m maximum depth). About 40% of the lake-bed area is covered by submersed and floating-leaved macrophytes during the growing season (Carter et al. 1997).

Micrometeorological sensors were mounted on a small communications tower that was inserted into lake sediments, approximately equidistant from the northwest, southwest, and northeast shores. The tower was guy-wired underwater to make it a stationary platform for eddy covariance instruments, which were mounted 1.2 m above the lake. Sensors at this height were within the equilibrium boundary layer (lowest 10% of the internal boundary layer, where fluxes may be assumed constant) as determined from Kaimal and

Table 1. List of measurement periods and instrumentation.*

Period	CO ₂	Water vapor	Temperature	Vertical wind	Friction velocity
11–18 Apr 92 (thaw 6 Apr)	ADI-IRGA	ADI-IRGA	ATI-Sonic	ATI-Sonic	ATI-Sonic
25–26 Apr 93 (thaw 15 Apr)	ATDD-IRGA	ATDD-IRGA	CSI-Sonic	CSI-Sonic	Modeled
27–29 Jul 93	LiCOR-IRGA	CSI-Krypton	CSI-Sonic	CSI-Sonic	Modeled
12–14 Oct 93	LiCOR-IRGA	CSI-Krypton	CSI-Sonic	CSI-Sonic	Modeled
18–25 Apr 94 (thaw 16 Apr)	LiCOR-IRGA	CSI-Krypton	CSI-Sonic	CSI-Sonic	Modeled

* ADI, Advanet Inc., Okayama, Japan; 15-cm open sensing path; ATI, Applied Technologies Inc., Boulder, Colorado; ATDD, Atmospheric Turbulence Diffusion Division, Oak Ridge, Tennessee (Auble and Meyers 1992); 15-cm open sensing path; CSI, Campbell Scientific Inc., Logan, Utah; LiCOR, LiCOR Corporation, Lincoln, Nebraska; this closed-path system including the IRGA operated with a 6 liter min⁻¹ flow rate, 6 m of 6.2-mm-diameter stainless steel tubing, and a temperature-controlled water bath, as described in Suyker and Verma (1993); IRGA, Infrared Gas Analyzer.

Finnigan (1994, eq. 4.5) for the tower location under these conditions: neutral stability, 3–5 m s⁻¹ winds, 0.001-m roughness length, and 300-m fetch. The depth of the equilibrium boundary layer increases with increasing atmospheric instability, surface roughness, and fetch. South winds were associated with the least fetch.

Instrumentation—Fluxes of CO₂, water vapor, heat, and momentum were measured using eddy covariance instruments oriented into the prevailing wind direction. Table 1 lists instruments used during the five measurement periods from April 1992 to April 1994. All sensors had a frequency response of at least 10 Hz. Data logging hardware, calibration gases, and power supplies were contained on a small, inflatable raft tethered to the tower and allowed to swing downwind. Deep-cycle batteries provided electrical power, allowing eddy covariance measurements to be made for several hours a day.

Downwelling solar radiation and photosynthetic photon flux density (PPFD) were measured at 2.4 m above the lake with quantum sensors (model PSP, Eppley Labs; LI-190Si, Li-Cor). Mean wind direction and speed were measured at 2.4 m on the tower with a directional vane and cup anemometer (model 03001 Wind Sentry, Campbell Scientific). Mean temperature and humidity were measured with a temperature–humidity probe (model HMP 35C, Campbell). Water temperature was measured with thermocouples at 0.05, 0.25, 0.5, 0.75, 1, 1.5, 2, 2.5, 3, 4, 5, 6, 7, 8, and 9 m depths at the tower location. All non-eddy covariance-related measurements were recorded on a separate data logger (model 21x, Campbell). Averages of these measurements were computed at the end of each half-hour, except water temperature, which was scanned once each half-hour. Wind speed, air temperature, humidity, and water temperature, averaged over hourly intervals, were also measured at the lake roughly 200 m east of the tower location on a semi-permanent raft (Sturrock et al. 1992). These data were used in the intervals between lake thaw and the beginning of tower measurements to make model forecasts of CO₂ flux.

The following procedures were used to measure [CO_{2, aq}]: In April 1992, 50-ml polypropylene syringes were filled with water from 0.1, 1, 2, 3, 4, 5, 6, 7, 8, 8.5, and 9 m depths within 50–100 m of the tower. Half of the water sample was evacuated and replaced with 25 ml of air with a known CO₂ concentration. The air–water mixture was vigorously agitated for 3 min to achieve air–water CO₂ equilibration in the syringe headspace. The air was extracted and injected into a

gas chromatograph having a flame-ionization detector and methanizer. The same procedures were followed in 1993 (except that no samples were analyzed in April). Temperatures of the in situ water and equilibrated water samples at the time of analysis were recorded and used to calculate in situ gas concentrations following Plummer and Busenberg (1982). In April 1994, the air sample was injected into an infrared gas analyzer (IRGA model EGM, PP Systems) instead of the gas chromatograph. In July 1993, CO₂ was also measured using an air–water equilibrator apparatus similar to that described in Womack and Crawford (1991).

Computations—Fluxes were computed from recorded time series of eddy covariance instrument signals. Tri-axis anemometer signals were coordinate rotated into the mean wind stream following procedures in Kaimal and Finnigan (1994). All fast-response signals used to compute F_c were detrended using a digital recursive filter (200-s time constant; McMillan 1988). F_c and water-vapor fluxes derived from the open-path sensor were computed from the appropriate covariances after adjustment for temperature- and humidity-induced density fluctuations (Webb et al. 1980, Kramm et al. 1995). For its greater accuracy, we chose Kramm et al.'s adjustment formula, which we found to be about 2/3 that of Webb et al.'s for a latent heat flux of 100 W m⁻². Density variations led to an uncertainty in F_c, measured with the open-path sensor, of about 0.46 μmol m⁻² s⁻¹ when the uncertainties in sensible heat flux and latent heat flux were 10 W m⁻² each. Ambient temperature fluctuations in the closed-path system were effectively dampened by the heat exchanger (sample air temperature variance <0.05°C as determined from an in-stream thermocouple). Therefore, the uncertainty in F_c in this case (0.07 μmol m⁻² s⁻¹) was solely due to uncertainty in the latent heat flux measurement. IRGA cross-sensitivity to CO₂ and water vapor was adjusted following Leuning and Moncrieff (1990). Underestimates of flux due to sensor separations, frequency response, and volume averaging were made using an algorithm by Moore (1986). Underestimates due to damping of CO₂ concentration fluctuations in the closed-path sampling tube were recovered following Leuning and Moncrieff (1990). The CO₂ time series was adjusted for the delay (relative to the other instruments) caused by the gas travel time through the sampling tube to the IRGA, employing the procedure discussed in Fan et al. (1992). Water-vapor density measured with the krypton hygrometer was adjusted for oxygen absorption (Tanner et al. 1993). All latent heat flux calculations were

adjusted for the effects of temperature fluctuations on air density (Webb et al. 1980).

A signal spike (defined as a point-to-point change >5 V in raw voltage) search-and-removal subroutine monitored each half-hour run for quality. Time series of most runs were visually inspected. Additionally, velocity and scalar spectra and cospectra were computed on all runs. Runs were rejected if more than 100 spikes were detected (0.5% of the time series) or if the spectra and cospectra did not express an inertial subrange slope (Kaimal et al. 1972).

The complete eddy covariance instrument and data logging system was tested in the laboratory to determine the minimum resolvable flux above signal noise. A CO_2 gas standard of 350 ppm was run through the Li-Cor 6252 IRGA, and the single-axis sonic anemometer was enclosed in a sealed box containing still air. The 'zero flux' calculated from the covariance of CO_2 concentration and vertical velocity indicated a system noise of $\pm 0.055 \mu\text{mol m}^{-2} \text{s}^{-1}$ from five half-hour runs.

In periods immediately after the lake thawed, F_c was also estimated from changes in lake-volume storage of dissolved CO_2 —hereafter referred to as the storage method flux. Lake storage of CO_2 at time t was calculated from Eq. 7:

$$C_t = \sum_{i=1}^n [\text{CO}_{2\text{aq}}]_i A_i (D_{1/2(i+1)} - D_{1/2(i-1)}), \quad (7)$$

where A_i is the lake area at the depth D_i from which water was extracted to determine the equilibrated CO_2 concentration $[\text{CO}_{2\text{aq}}]_i$. Depth increases with the index. Volume slices are vertically bounded by $\frac{1}{2}$ the distance between sampling depths, except for $i = 1$, where $D_{1/2(i-1)} = 0$. The flux from the lake's surface (area, A_0) over the time between measurements (Δt) is

$$F_c = \frac{(C_{t-1} - C_t)}{\Delta t A_0}, \quad (8)$$

where the index increases with time. We assumed that the change in storage was due to lake-atmosphere exchange (Michmerhuizen et al. 1996). We also assumed that degassing events were dynamic enough to discount mechanisms associated with HCO_3^- conversion and dissolved organic carbon (DOC) consumption. Because storage change calculations in this study covered no more than weekly exchanges and were made in early spring when the photosynthetic sink relative to $\text{CO}_{2\text{aq}}$ storage is likely very small, we believe this assumption to be reliable. Lake-water residence time due to groundwater interaction is ~ 4 yr (LaBaugh et al. 1995); therefore, hydrologic exchange of CO_2 was assumed to be negligible.

We compared our measured values of flux with three different models: homogeneous boundary layer (Deacon 1977, 1981; using Eqs. 2 and 3 with $Sc_t = 1$, $\alpha = 0.082$, $\beta = \frac{2}{3}$), modified homogeneous boundary layer (Deacon 1981; Wesely et al. 1982; with $Sc_t = 1$, $\alpha = 0.082$, $\beta = \frac{1}{2}$), and Soloviev and Schlusel's (1994, 1996) surface-renewal model (truncated version, using Eqs. 2 and 6). All three models require values for u_* and skin temperature. Equations for u_* and surface velocity were adapted from work by Bourassa et al. (1999). Skin temperature was computed from near-

surface bulk water temperature. Values of Δt were computed from the right side of Eq. 5 for nighttime conditions and with additional formulae (Soloviev and Schlusel 1996) to include daytime heating of the skin by solar radiation. Both night and day conditions require measurements or estimates of sensible and latent heat fluxes and the radiation balance. Heat fluxes were computed using equations given in Clayson et al. (1996), while the radiation balance and absorption of solar radiation in the near-surface layer was computed following Fairall et al. (1996). Fairall's model requires input of measured solar radiation, temperature, and relative humidity, which are required for the long-wave radiation components. Measured wind direction and speed statistics are used in equations adapted from Alam and Curry (1997) for the development of water-body states that define fetch-dependent wave characteristics. Wave characteristics, in turn, describe surface roughness, which affects u_* and surface fluxes. Values for Pr , Sc , Rf_0 , and Ke were also updated during each model iteration. For comparison, we ran Wick et al.'s (1996) model for skin temperature, which we found to vary little from predictions of the Soloviev and Schlusel (1994) model, at least within the environmental conditions of our study. Surface heat fluxes and u_* predicted from the combination of these models closely matched the measured data, as we will show in a forthcoming paper.

Results and Discussion

Measurements after lake thaw— F_c values immediately after lake thaw were expected to be the largest and most dynamic of the year. While the lake is covered with ice (usually November through April), a substantial amount of dissolved CO_2 derived from heterotrophic respiration evolves in bottom sediment around decaying vegetation. When the surface thaws, lake turnover mixes high- $[\text{CO}_{2\text{aq}}]$ benthic water through the water column. This results in large lake-atmosphere $[\text{CO}_2]$ differences and potentially in large lake-atmosphere F_c (Michmerhuizen et al. 1996).

We began measurements as soon after lake thaw as feasible (Table 1). Results are presented for the springs of 1992 and 1994, since no concurrent lake-water $[\text{CO}_{2\text{aq}}]$ measurements were obtained in 1993. Trends in mean wind speed, air and water temperatures, $[\text{CO}_2]$ concentrations, and CO_2 storage are plotted in Figs. 2–3. In both years there were notable diurnal trends in mean wind speed and air temperatures. Near-surface water temperatures gradually warmed during the measurement period, with small diel variations. Although atmospheric $[\text{CO}_2]$ remained fairly steady (15.6–16.4 mmol m^{-3}), lake-water $[\text{CO}_{2\text{aq}}]$ and $\text{CO}_{2\text{aq}}$ storage tended to exponentially decrease with time. Initial surface-water $[\text{CO}_{2\text{aq}}]$ and storage magnitudes were about three times larger in 1992 (Fig. 2c) than in 1994 (Fig. 3c), possibly resulting from greater biological activity in the 1991 growing season that provided a larger quantity of decayed biomass. Also, although $[\text{CO}_{2\text{aq}}]$ and storage data exhibited a smooth exponential decline with time, the decline in 1992 was more erratic. During the first 3 d after thaw in 1992, storage increased from 330 to 450×10^3 mol. This may have been caused by enhanced mixing of $\text{CO}_{2\text{aq}}$ from sediment pore

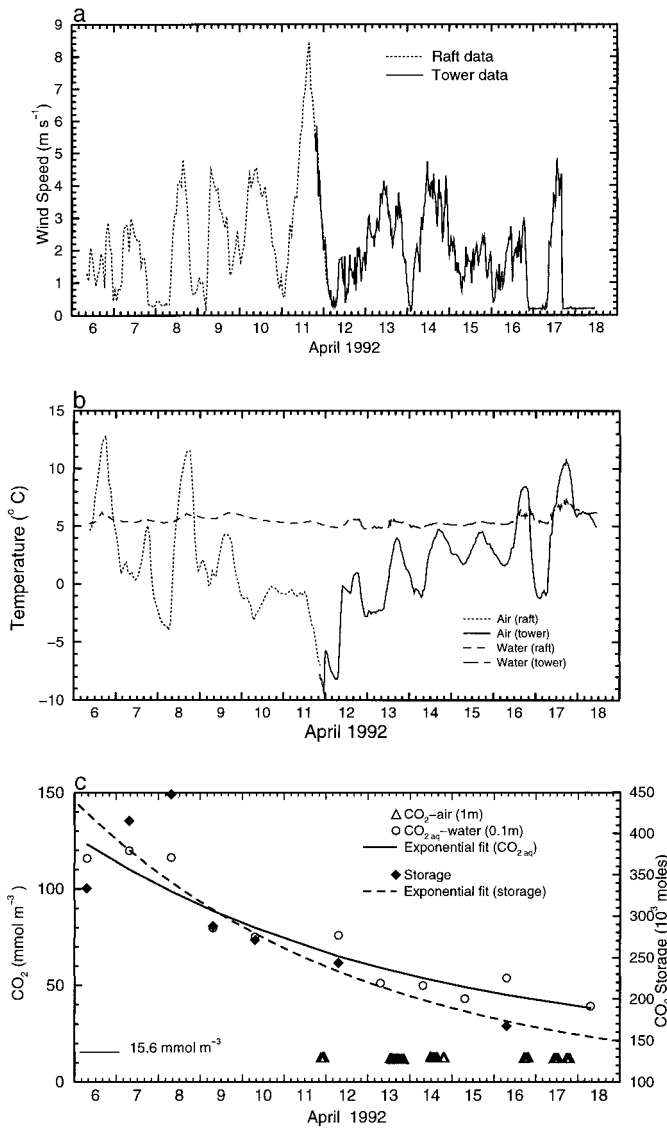


Fig. 2. (a) Average wind speed at 2.4 m above the lake, April 1992. (b) Average air temperature (2 m above the lake) and water temperature (0.05-m depth). (c) Average partial pressure of CO₂ in air at a 1-m height, [CO_{2, aq}] in surface water, and [CO_{2, aq}] lake storage. Fitted curves are [CO_{2, aq}] = 16.6 + 114.6 exp(-.142[Day-6]), $R^2 = -.94$, and Storage ($\times 10^3$) = 100 + 340.3 exp(-.149[Day-6]), $R^2 = -.95$. $P < 0.01$ for both regressions.

water to benthic water by wind-induced circulation. This phenomenon was not seen in spring 1994.

Temperature profiles of the lake-water column in spring 1992 were nearly isothermal through the observation period, varying $<1^\circ\text{C}$ with depth from 0.1 to 9 m. By 16 April 1992, there was evidence of thermal stratification and the development of a thermocline. By contrast, air temperatures were generally warmer in April 1994, leading to warmer lake-water temperatures and more pronounced day-to-day changes in temperature profiles. In 1994, lake thaw occurred on 16 April, followed by lake turnover and isothermal conditions until the appearance of a thermocline on 20 April.

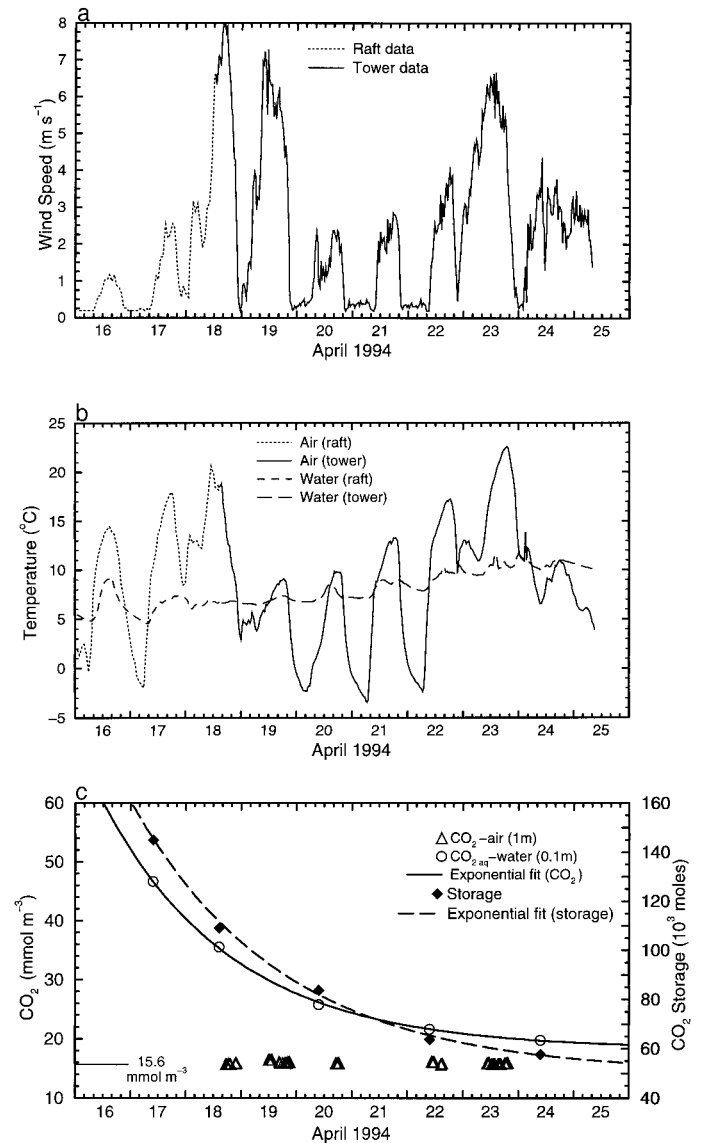


Fig. 3. (a) Average wind speed 2.4 m above the lake, April 1994. (b) Average air temperature (2 m above the lake) and water temperature (0.05-m depth). (c) Average partial pressure of CO₂ in air at a 1-m height, [CO_{2, aq}] in surface water, and [CO_{2, aq}] in lake storage. Fitted curves are [CO_{2, aq}] = 16.6 + 44.3 exp(-.428[Day-16.5]), $R^2 = -.99$ and Storage ($\times 10^3$) = 50 + 109.1 exp(-.366[Day-16.5]), $R^2 = -.99$. $P < 0.01$.

Shapes of [CO_{2, aq}] profiles for both years (Figs. 4a,b) displayed small increases in [CO_{2, aq}] with depth, suggesting that dissolved gas was well mixed from the surface down to the vicinity of benthic waters. Changes with time in the concentration of the total column were greatest early in the measurement period. The profiles occasionally exhibited kinks (17–18 April 1994), where concentrations at 4 m were markedly higher than at either deeper or shallower depths.

Figures 5 and 6 illustrate a comparison between eddy covariance and storage-method fluxes (calculated two different ways). Storage-method (raw) fluxes derived from the differences between observations in whole-lake [CO_{2, aq}] storage

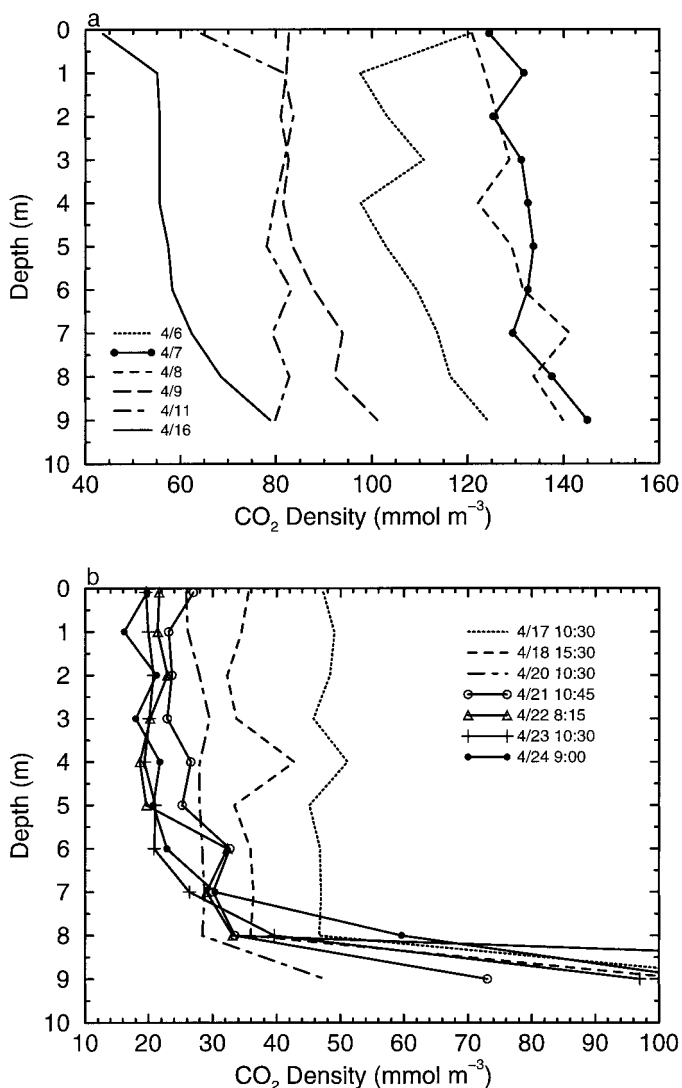


Fig. 4. (a) Lake $[\text{CO}_{2\text{aq}}]$ profiles with depth, April 1992. (b) Lake $[\text{CO}_{2\text{aq}}]$ profiles with depth, April 1994.

are plotted as histograms. Flux was assumed to be constant between observations, yielding a step-like pattern. Since $[\text{CO}_{2\text{aq}}]$ storage exhibited an exponential decay with time (Figs. 2c, 3c), we fit storage data with an exponential function to yield a somewhat more realistic pattern of flux magnitude. All three sets of estimates plotted in the figures indicate the same general, decreasing trend of flux with time. Half-hourly eddy covariance measurements in April 1992 varied considerably between days and over the period of observation, ranging from 2.3–2.7 $\mu\text{mol m}^{-2} \text{s}^{-1}$ on 11 April (Fig. 5), coincident with a very large measured air–water $[\text{CO}_2]$ difference ($>45 \text{ mmol m}^{-3}$), to values near zero by 17 April. Flux estimated from raw $[\text{CO}_2]$ data using the storage method peaked near 5.0 $\mu\text{mol m}^{-2} \text{s}^{-1}$ on 8–9 April, dropping to about 10% of these values by 16 April. However, using the exponential fit to storage data (Fig. 2c), a much smaller range in flux was seen. Peak F_c for 8–9 April was about 1.0 $\mu\text{mol m}^{-2} \text{s}^{-1}$, dropping to values comparable with those computed from raw storage data by 16 April.

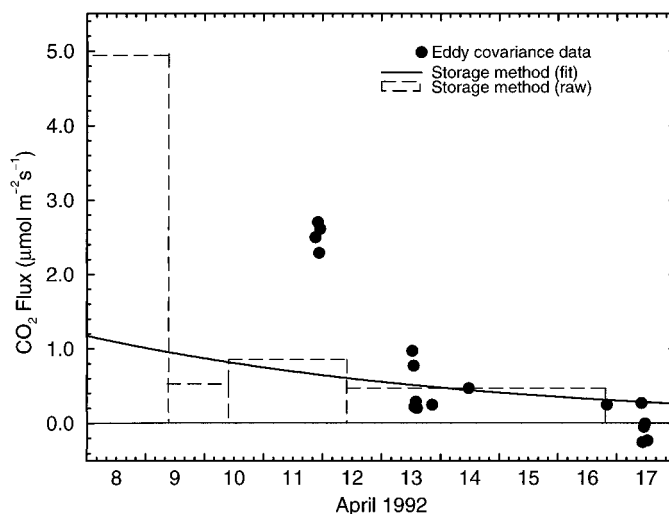


Fig. 5. April 1992 temporal trends of CO_2 flux measured with eddy covariance and storage change methods.

Intraday eddy covariance measurements of F_c in April 1994 (Fig. 6) also revealed considerable variation in flux (0.15–0.6 $\mu\text{mol m}^{-2} \text{s}^{-1}$ on 18 April and 0.25–0.8 $\mu\text{mol m}^{-2} \text{s}^{-1}$ on 19 April) when measured air–water $[\text{CO}_2]$ differences were $<15 \text{ mmol m}^{-3}$.

In April 1993, lake-water $[\text{CO}_{2\text{aq}}]$ was not measured and eddy covariance measurements began 10 d after lake thaw. For a 3-d period, mean flux averaged 0.11 $\mu\text{mol m}^{-2} \text{s}^{-1}$ (SD, ± 0.61). Small efflux would be expected 10 d postthaw, given the trends of 1992 and 1994 data.

Comparison of transfer velocities derived from measurements and models—Measured values of F_c from eddy covariance, C_w , and C_a were used in Eq. 2 to compute V_B (mass transfer velocity) that could be compared to results from the homogeneous boundary-layer and surface-renewal models. Values for C_w were derived from an exponential fit of

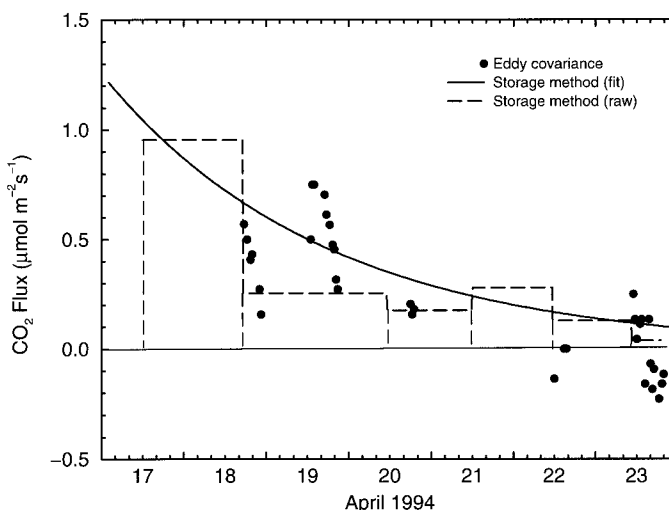


Fig. 6. April 1994 temporal trends of CO_2 flux measured with eddy covariance and storage change methods.

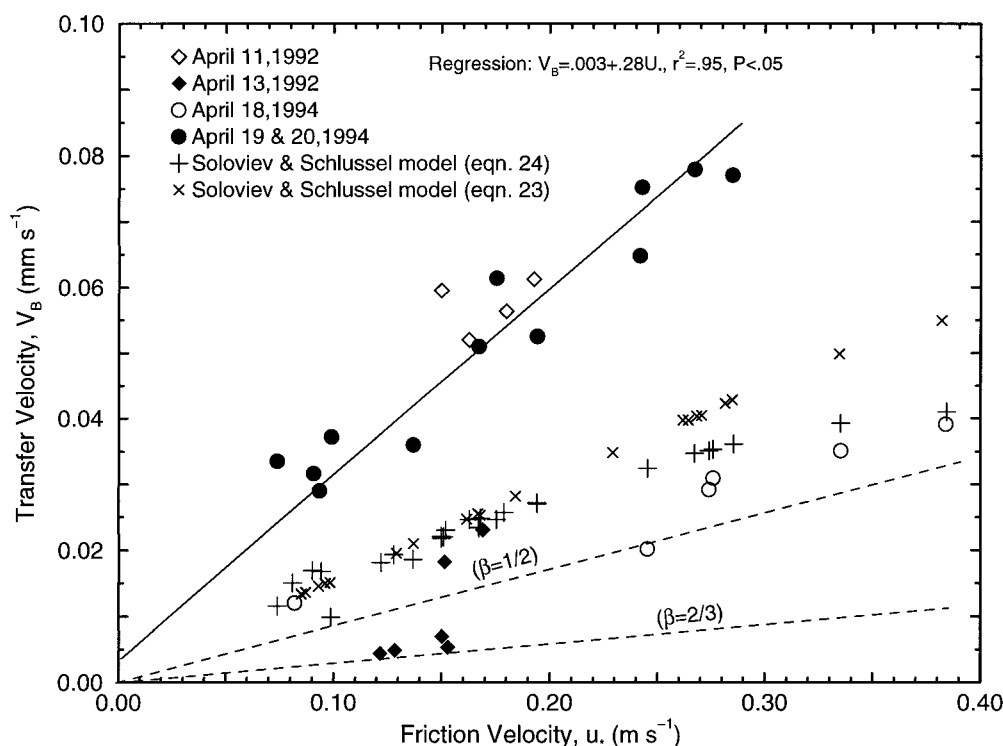


Fig. 7. Measured and predicted dependence of transfer velocity for CO₂ on friction velocity in air. These data are from the first days of measurement in each year. Predicted values are from Soloviev and Schlusel's (1994, 1996) surface-renewal model and from the homogeneous boundary-layer model (dashed lines). Values from the latter model were computed with a fixed temperature of 5°C and values for β as indicated above the dashed lines.

[CO_{2, aq}] measured at 0.1-m depth to the elapsed time since ice-out. C_a was held constant at the average measured value of 16 mmol m⁻³. Because [CO_{2, aq}] was measured as [CO_{2, air}] in the equilibrated gas headspace in the sample syringes, S in Eq. 2 was set to 1. Data points for the first days of measurement in both 1992 and 1994 were plotted versus u_* (Fig. 7). (Note that u_* was measured in 1992 but modeled in 1994.) Eddy covariance data presented in Fig. 7 were selected when wind direction ranged $<30^\circ$ and wind speed was >2 m s⁻¹. Values of V_B versus u_* computed for the homogeneous boundary-layer models ($\beta = 2/3$, $\beta = 1/2$, $Sc_t = 1$) and Soloviev and Schlusel's (1994, 1996) surface-renewal model are also shown. In addition, the Soloviev and Schlusel model was run in its nontruncated state (left sides of Eq. 5 and 6), indicating that the truncated version substantially departs from the full model at progressively larger u_* (up to 15% at $u_* = 0.4$). Regarding the homogeneous boundary-layer models, although there is some uncertainty in the value of Sc_t (range, 0.7–1; Deacon 1981), a value of 0.7 would have only led to an increase of about 11% in estimates of V_B .

Measured V_B values fell into three sets. A set of four points measured on 13 April 1992 lay along the $\beta = 2/3$ boundary-layer model prediction. The second set (13 April 1992 and 18 April 1994) lay nearest the surface-renewal model predictions. The third and largest set (11 April 1992 and 19–20 April 1994) was distinct from the other measured groups. V_B for this set was about three times the value pre-

dicted by the homogeneous boundary-layer model ($\beta = 1/2$) and about 2–2½ that of the surface-renewal models. Another notable characteristic of the three sets of data was that, except for two points from the 13 April 1992 data set, there was a consistent intraday relationship between V_B and u_* . As noted earlier, larger discrepancies between eddy covariance and homogeneous boundary-layer model estimates of V_B were systematically seen by Wesely et al. (1982), Smith and Jones (1985) and Crawford et al. (1993) over oceanic coastal waters. In contrast, Denmead and Freney (1992), working over an artificial freshwater pond, often found agreement between aerodynamic profile measurements of F_c and the homogeneous boundary-layer model ($\beta = 1/2$). Data shown in Fig. 7 indicate that there are temporal mechanisms determining when models and measurements agree.

In analyzing the discrepancy between modeled and measured transfer velocity in the present study, we considered the possible influence of a variety of factors related to measurement methodology and environmental conditions that might introduce either systematic or random errors. To reduce the relative significance of measurement error, we chose data from periods of large air–water [CO₂] differences and large F_c . Errors in flux measurement derived from noise and those associated with adjustments to flux, combined with errors associated with determining air–water [CO₂] differences, translated to a relative V_B error of 0.0031 mm s⁻¹ (1992 data) and 0.0036 mm s⁻¹ (1994 data). When V_B was calculated from measurements, some error may have oc-

Table 2. Environmental conditions corresponding to data depicted in Fig. 7.*

Date	Time (h:min)	V_B (mm s ⁻¹)	$[C_w/S] - C_a$ (mmol m ⁻³)	F_c ($\mu\text{mol m}^{-2} \text{s}^{-1}$)	u^* (m s ⁻¹)	T_a (°C)	T_w (°C)	R solar (W m ⁻²)	Wind direction (degrees)
11 Apr 92	21:00	0.056	43.9	2.46	0.180	-7.79	5.20	0	332
	22:00	0.061	44.3	2.70	0.196	-8.13	5.21	0	317
	22:30	0.052	43.5	2.26	0.162	-8.58	5.21	0	319
	23:00	0.060	43.6	2.62	0.150	-8.52	5.20	0	307
13 Apr 92	12:30	0.023	41.7	0.96	0.172	0.48	5.49	456	197
	13:00	0.018	42.2	0.76	0.153	1.32	5.27	518	206
	13:30	0.0054	40.7	0.22	0.154	1.72	5.67	456	205
	14:00	0.0070	41.4	0.29	0.151	2.08	5.35	347	194
	14:30	0.0049	40.8	0.20	0.127	2.59	5.33	389	186
	21:00	0.0046	41.3	0.19	0.123	2.05	5.33	0	191
18 Apr 94	17:30	0.039	13.3	0.52	0.384	14.70	6.68	81	326
	18:00	0.035	14.0	0.49	0.335	13.40	6.75	278	325
	19:00	0.029	13.8	0.40	0.274	12.49	6.78	186	327
	19:30	0.031	13.9	0.43	0.276	11.50	6.87	104	326
	21:30	0.020	13.5	0.27	0.245	9.18	6.83	0	325
	22:00	0.012	13.3	0.16	0.082	8.60	6.77	0	316
19 Apr 94	13:00	0.077	9.6	0.75	0.284	7.03	6.88	873	304
	13:30	0.078	9.5	0.75	0.267	7.40	6.96	882	313
	16:30	0.075	9.3	0.70	0.243	8.50	7.21	638	313
	17:00	0.065	9.3	0.61	0.241	8.88	7.26	566	310
	18:30	0.061	9.2	0.57	0.175	9.12	7.40	289	311
	19:00	0.053	8.9	0.48	0.194	9.00	7.36	196	319
	19:30	0.051	8.8	0.45	0.167	8.83	7.38	113	313
	20:00	0.036	8.7	0.32	0.137	8.24	7.34	37	318
	20:30	0.032	8.4	0.27	0.091	7.44	7.21	6	314
20 Apr 94	17:30	0.037	5.4	0.20	0.099	9.83	7.82	222	281
	18:00	0.029	5.4	0.16	0.093	9.82	7.55	114	274
	18:30	0.033	5.4	0.18	0.074	9.74	7.46	96	264

* V_B is transfer velocity derived from flux and CO₂ concentration measurements; $[C_w/S] - C_a$ is the water-air CO₂ concentration difference, where C_w is measured at 1.15 m and C_a is derived from the exponential fit of CO₂ concentration measurements of water at 10 cm below the surface (see Figs. 2c, 3c); F_c is CO₂ flux; u^* is friction velocity; T_a is air temperature at 2 m; T_w is water temperature at 5 cm; R solar is shortwave radiation; and wind direction was measured at 2.4 m.

curred with our assumption of a smooth, nonlinear decay of $[CO_{2, \text{aq}}]$ for 1992 data, owing to substantial scatter in $[CO_{2, \text{aq}}]$ measurements about the exponential fit (Fig. 2c). However, data from 1994 were very consistent with time and are well described by the exponential fit (Fig. 3c).

Regarding measurement methodology, data in sets 2 and 3 were derived from different instruments having different calibration equations, corrections, and data archiving and computation software. Both groups contain data from different days, years, and chronological sequences. It is unlikely that systematic errors in measurement methodology would be duplicated across different hardware and software.

Next, we examined bioenvironmental factors. The influence of chemical or biological activity on air-water F_c is documented in the literature (Smith 1985, Schindler et al. 1997). Although we did not measure them, neither was suspected to have substantially influenced flux. For instance, the sharp decline in profiles of $[CO_{2, \text{aq}}]$ from about the 1-m depth to the surface on 11 and 16 April 1992 (Fig. 4a) suggested the possibility of biological uptake of CO₂, while the 20 April 1994 profile (Fig. 4b) was basically flat. However, data from both 11 April 1992 and 20 April 1994 appear in the same set of points in Fig. 7. The model versus measured V_B

discrepancy repeated itself in 1994, but was reversed (large V_B occurred early in 1992 but late in 1994) such that, when summed over both years, sets 2 and 3 contain points from a range of environmental conditions (Table 2).

We did not find possible explanations for large V_B through a dependency on fetch, flux footprint, or the determination of u^* . In the 1992 data set, both u^* and F_c were directly measured with eddy covariance. Kwan and Taylor (1994), in their model analysis of gas flux from lakes, point out from the literature that u^* gradually adjusts from its land value to one representative of water. We would expect therefore that under the worst-case fetch scenario (stable air), measured u^* would be contaminated to some extent by that adjusted to the land's boundary-layer, if the flux footprint extended beyond the shoreline. Since u^* over water (a smoother surface) would be less than that over land, measured u^* would be larger than expected over water. Additionally, F_c in early spring (before leafing of the surrounding forest) would more likely be contaminated by low upward-directed F_c over land, arising from soil respiration. Measurements in a north-temperate deciduous forest by Wofsy et al. (1993) indicate a forest floor efflux (F_c) of about 0.2 $\mu\text{mol m}^{-2} \text{s}^{-1}$ in early spring. The combination of larger-than-expected u^* and low-

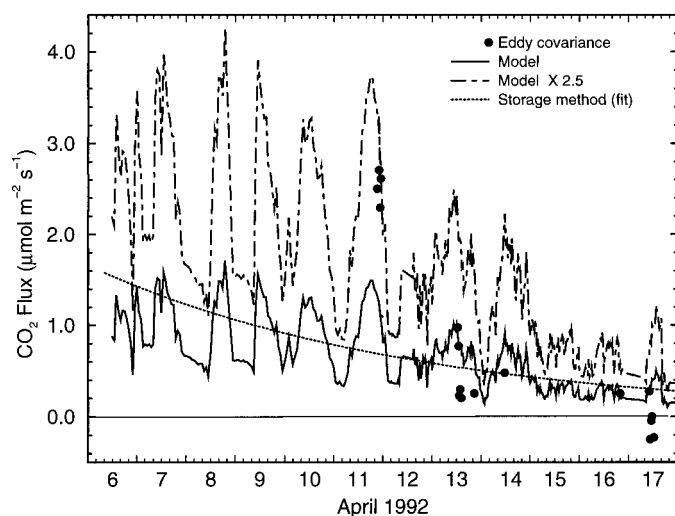


Fig. 8. Variation of measured and modeled (Soloviev and Schlussel 1994) lake-atmosphere CO₂ flux with time (April 1992).

er F_c would lead to lower-than-expected transfer velocity—counter to the direction needed to explain the model versus data discrepancy. In 1994, F_c was again directly measured, but u_* was modeled. If actual u_* was larger than that modeled, measured V_B would be larger than modeled. However, comparisons of modeled and measured u_* in 1992 agreed within $\pm 20\%$, while V_B differed by a factor of 2. In addition, we found both 1992 and 1994 data in both sets (2 and 3). No strikingly different meteorological conditions or water temperatures appeared between the groups of points (Figs. 2a,b and 3a,b; Table 2). However, in all cases, the larger-than-predicted V_B coincided with periods following strong winds and rapidly falling temperature, and only when the water temperature was greater than that of air. Bubble-aided transfer due to breaking waves (Wallace and Wirick 1992) would be an unlikely mechanism for large V_B for most of the data, since breaking waves were seldom observed when large V_B occurred. Note that large V_B were also measured when u_* was small.

Finally, as noted in the Theoretical Background section, we are aware that capillary waves enhance air-water gas flux. Jahne et al. (1987) discuss the occurrence of enhanced gas transfer as the water surface changes from a rigid (no waves) to a free surface (waves) in which β coincidentally changes from $\frac{2}{3}$ to $\frac{1}{2}$. This may be an important mechanism describing the magnitude of V_B for the lowest u_* values reported in Fig. 7. At larger u_* , Jahne et al. also mention that, at times, higher gas exchange rates were observed in experimental wave tanks. More recently, Szeri (1997) estimated that capillary waves may enhance gas transfer by several to a few tens of percent of the flux predicted by surface-renewal models. The extent of enhancement depends on capillary wave structure, but under extreme conditions the enhancement may be as large as 60–70%. Unfortunately, we cannot evaluate the possibility of enhanced flux due to capillary wave structure, since regular quantitative assessments of the wave field were not made.

In summary, while we have considered a number of possible causes for the discrepancy between data and models in

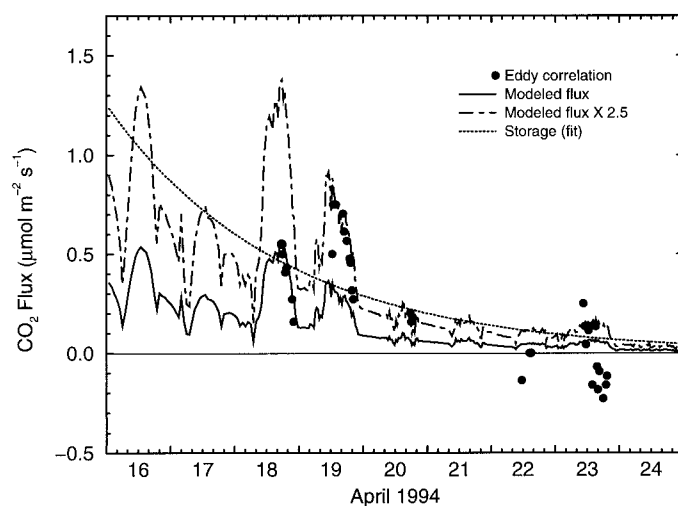


Fig. 9. Variation of measured and modeled (Soloviev and Schlussel 1994) lake-atmosphere CO₂ flux with time (April 1994).

the u_*-V_B relationship, we have not found a provable or consistent explanation.

Comparison of measured and modeled fluxes—Eddy covariance and storage method fluxes were compared with the surface-renewal model (Soloviev and Schlussel 1994, 1996; truncated version) for the full period of record in April 1992 (Fig. 8) and April 1994 (Fig. 9). Also graphed is the surface-renewal model output multiplied by a factor of 2.5, which is the approximate difference between the V_B measured versus that modeled for the group of measured points fitting the regression line in Fig. 7. As shown in the analysis of transfer velocities from the first 2 d of eddy covariance measurements, the surface-renewal model agreed well with eddy covariance measurements on some days but underestimated flux by about 2.5 times on other days. In comparison, flux derived from the storage method suggested a flux somewhere between the modeled flux and 2.5 times that.

Modeled (surface renewal) cumulative F_c was compared to that computed from the exponential fits to storage data (Figs. 2c, 3c) in Fig. 10. Cumulative storage flux is the summation of F_c ($\mu\text{mol m}^{-2} \text{s}^{-1}$) over time, yielding a mass per unit area. Figure 10 shows a marked interannual variability in flux rates and cumulative flux. By Day 13 postthaw in 1992, 90% of the cumulative flux had occurred. This amounted to 0.76 mol m^{-2} or $2.8 \times 10^5 \text{ mol}$ for the entire lake surface area. In contrast, much less CO₂ was released in 1994 (0.28 mol m^{-2}), when 90% of cumulative flux was attained at 9 d postthaw. This is roughly $\frac{1}{3}$ of the 1992 release.

Modeled flux compares well with that derived from the storage method in both trends and magnitudes during 1992, but not in 1994, when significant differences occurred early in the measured period. The model predicted a cumulative flux of 0.62 mol m^{-2} by Day 13 in postthaw 1992, compared to a measured value of 0.78 mol m^{-2} . In 1994, we saw a sizable underestimate: modeled flux was 0.12 mol m^{-2} by Day 9, versus 0.29 mol m^{-2} estimated from storage measurements on that day.

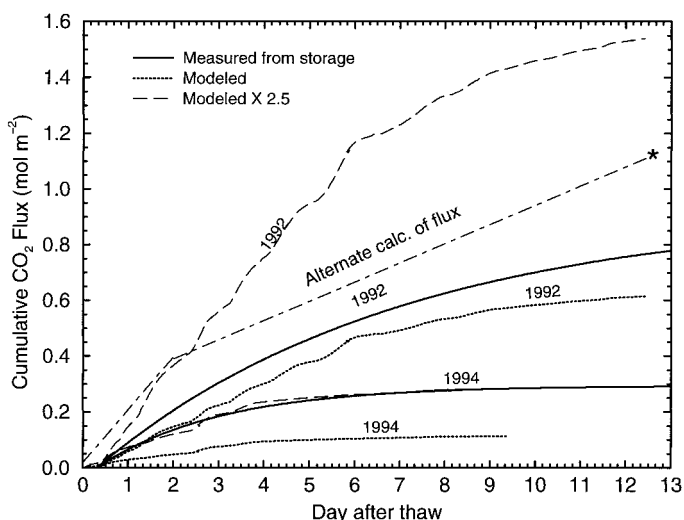


Fig. 10. Cumulative CO_2 flux distribution with time after lake thaw (thaw represented at origin). Predictions are from Soloviev and Schlüssel (1994) surface-renewal model.

Model calculations of cumulative flux with a 2.5 times V_B were also compared to storage method results (Fig. 10), showing excellent agreement between measured and modeled values in 1994. This exercise led to a total cumulative flux of 1.54 mol m^{-2} for 1992—a large overestimate. In 1992, $\text{CO}_{2\text{aq}}$ storage (Fig. 2c) increased during the first 2 d of measurement. If these storage data were accurate, total $\text{CO}_{2\text{aq}}$ storage loss was considerably larger than estimated from the exponential curve fitted to storage data. Following this observation, we made an alternative estimate of possible total flux based on measurements. First, we assumed a steady loss of $1 \times 10^5 \text{ mol CO}_{2\text{aq}}$ for 6–8 April, which was derived from the exponential curve for this time interval (Fig. 2c). To this was added the measured increase of $1 \times 10^5 \text{ mol}$ on 6–8 April, plus the loss from 8 through 18 April (about 2

$\times 10^5 \text{ mol}$). Summing the contributions, we found the total loss for the lake from 6 to 18 April to be about $4 \times 10^5 \text{ mol}$. After dividing by lake area ($37.09 \times 10^4 \text{ m}^2$), we obtained a cumulative loss of 1.1 mol m^{-2} , which lay halfway between the model and $2.5 \times$ model predictions, as indicated in Fig. 10.

Measurements during summer and fall—Measurements were obtained for a 12-h period (0800–2000 h) on 29 July 1993 during a warm, clear day. Air temperature rose from 16°C at 0800 h to 24°C at 1830, dropping to 23°C at 2000 h. Water temperature at 0.05 m steadily rose from about 22 to 22.5°C over the period. Wind speed was about $2\text{--}3 \text{ m s}^{-1}$ during 0800–1800 h, then trended downward. Eddy covariance measurements of F_c (averaging $-0.17 \mu\text{mol m}^{-2} \text{ s}^{-1}$) are shown in Fig. 11. Note that the y-axis for F_c has been inverted. F_c magnitude increased from near zero in the morning to a peak (maximum flux to the lake) after noon, before heading back through zero to positive values (flux to the lake) late in the day. Although measured flux is small, trends in F_c are not likely an artifact of the density adjustment to F_c , which could only originate from latent heat flux (LE). LE was large and trended upward, peaking in the afternoon. When entered into the air density adjustment to measured F_c , it reduced raw F_c magnitude in proportion to its own. Using the curve fit of F_c data and assuming that at night, with near-calm winds, flux is near zero, a 24-h average flux of $-0.09 \mu\text{mol m}^{-2} \text{ s}^{-1}$ was calculated. This compared well with the July monthly average of $-0.07 \mu\text{mol m}^{-2} \text{ s}^{-1}$ ($-2.3 \text{ mol m}^{-2} \text{ yr}^{-1}$ rate) that McConnaughey et al. (1994) estimated for the same lake in 1991. Present fluxes were obtained under clear skies (facilitating photosynthesis) and similar wind speeds. It is possible that downward F_c was caused by photosynthetic activity within the lake, although photosynthesis was not independently measured. The plot of PPFD indicates a peak in light intensity roughly coincident with the peak in F_c .

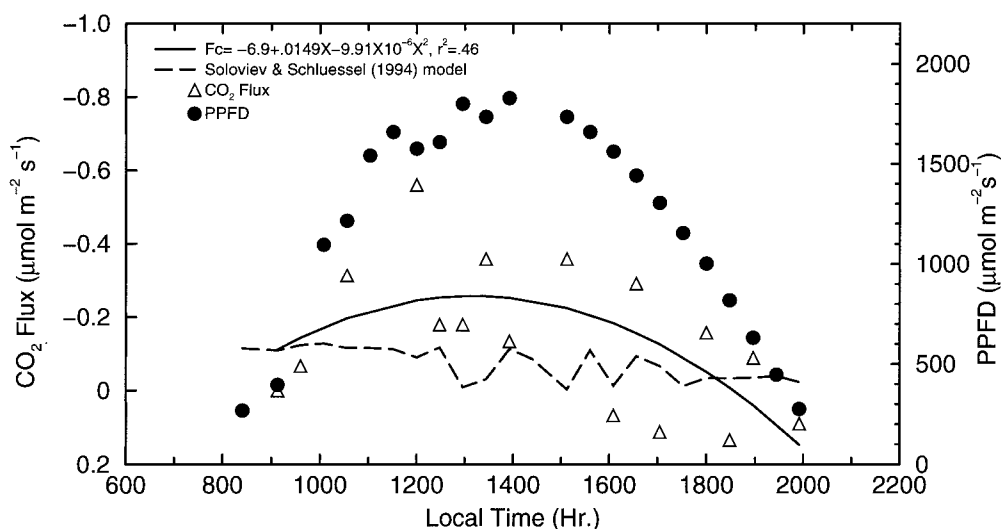


Fig. 11. Diurnal trends of CO_2 flux, photosynthetic photon flux density, and predicted CO_2 flux on 29 July 1993. Best-fit curve to measured CO_2 flux is $F_c = -6.9 + 0.0149 H - (9.91 \times 10^{-6} H^2)$, where H is the local time ($R^2 = .46$).

Our measurements of [CO_{2, aq}] near the tower averaged 3–4 mmol m⁻³ less than [CO₂] in air. The air–water [CO₂] difference at this location was too small to support the magnitude of the measured fluxes, even if the larger transfer velocities (2.5 times V_B) shown in Fig. 7 are applied. However, as discussed earlier, the lake surface area corresponding to the measured lake–atmosphere flux (the flux footprint) is upwind of the tower, possibly extending close to the shoreline on occasion. Measurements of [CO_{2, aq}] along transects to the shore in each cardinal direction revealed that surface waters in the littoral zone (up to 1/3 of the distance from shore to tower) were highly variable (2–13 mmol m⁻³ subatmospheric). The littoral zone was occupied by a substantial macrophyte population (Carter et al. 1997) that may represent a substantial sink for [CO_{2, aq}]. Summer subatmospheric [CO_{2, aq}] values are commonly found in productive lakes in North America, as documented by Hesslein et al. (1990).

Figure 11 also illustrates F_c values predicted by the surface-renewal model. We used the mean of the range of surface-water [CO_{2, aq}] values found from near-shore to the tower. Modeled flux averaged $-0.072 \mu\text{mol m}^{-2} \text{s}^{-1}$.

Eddy covariance measurements of F_c were made during a 3-d period from 12 to 14 October 1993. Although senescence of aquatic vegetation had occurred, lake [CO_{2, aq}] was still subatmospheric near the tower ($2.6 \pm 0.02 \text{ mmol m}^{-3}$). Daytime eddy covariance measurements made on 13–14 October averaged $-0.18 \mu\text{mol m}^{-2} \text{s}^{-1}$. The average modeled flux for the entire 3-d period was $-0.25 \mu\text{mol m}^{-2} \text{s}^{-1}$, or about $-2.1 \times 10^{-3} \mu\text{mol m}^{-2} \text{d}^{-1}$.

Conclusions

Unique sets of lake–atmosphere CO₂ flux (F_c) measurements were obtained during five periods spanning 3 yr. F_c was directly measured with eddy covariance equipment based on a stationary tower located near the center of a closed-basin lake. Additionally, in the springs of 1992 and 1994, F_c was independently estimated from the change in lake-volume storage of CO_{2, aq}. Combined, the F_c measurements quantified the magnitudes and temporal trends of lake–atmosphere CO₂ flux and transfer velocities. A surface-renewal model (Soloviev and Schlussel 1994, 1996) was used to predict flux for all periods, using meteorological data and the measured [CO₂] differences.

Springtime conditions immediately following lake thaw varied considerably in the magnitudes of F_c, surface-water [CO₂], lake-volume CO₂ storage, and meteorological conditions. On the first day of eddy covariance measurements in 1992 (5 d after lake thaw), F_c measured over 30-min intervals ranged between 2.3 and 2.7 $\mu\text{mol m}^{-2} \text{s}^{-1}$, coinciding with a daily average of 1.0 $\mu\text{mol m}^{-2} \text{s}^{-1}$ estimated from the storage method. Lake–atmosphere [CO₂] differences were >45 mmol m⁻³. In contrast, just 2 d after thaw in 1994, the lake–atmosphere [CO₂] difference was <15 mmol m⁻³. Measured flux ranged from 0.15 to 0.6 $\mu\text{mol m}^{-2} \text{s}^{-1}$, while storage method flux was about 0.7 $\mu\text{mol m}^{-2} \text{s}^{-1}$. In each instance, lake turnover had occurred before measurement, and evidence of a thermocline did not appear until near the end of the measuring period. Both measured and modeled

fluxes exhibited similar declining trends in F_c. Some notable day-to-day differences occurred between measured eddy covariance flux and that derived from the storage method. These differences are not systematic and remain unexplained. Differences were also apparent in measured and modeled comparisons of the CO₂ transfer velocity, V_B. Although there were occasions when either the surface renewal or, less frequently, boundary-layer models (Deacon 1977, 1981; Wesely et al. 1982) matched measured V_B, about as often, all models substantially underpredicted the measured V_B. Surface-renewal model predictions better matched measurements than the homogeneous boundary-layer models. The full surface-renewal model (Soloviev and Schlussel 1994, eqs. 21, 22) performed substantially better than its truncated form (Soloviev and Schlussel 1994, eqs. 25, 26) with increasing u_{*}.

The comparison of total cumulative CO₂ flux derived from lake-water storage change to that modeled also indicates that the surface-renewal model often underestimates measured flux. The amount of underestimate is not consistent. A small underestimate appears from 1992 data, when measured cumulative efflux reached 0.78 mol m⁻², while a large underestimate was found from the spring 1994 comparison, when total efflux reached 0.29 mol m⁻². Better agreement was found in cumulative flux comparisons and in comparisons with much of the eddy covariance data when transfer velocity was increased by a factor of 2½. This systematic correction greatly improved the overall comparison for April 1994 but not that for April 1992. However, April 1992 storage method derived flux is more uncertain than that of April 1994. From the existing data set, no explanation was found to address measured day-to-day variations in transfer velocity and discrepancies between cumulative fluxes derived from models and storage method approaches, although meteorological forcing through wind-wave interactions is suspected.

Eddy covariance measurements made in summer revealed a small but measurable downward flux during the day, tracking with the trend in solar radiation. In autumn, the magnitude of F_c was often below the detection limits of eddy covariance instruments. A small downward flux was estimated from model calculations.

In view of the uncertainty in predicting lake–atmosphere CO₂ transfer and its important global implications in air–water exchange, we strongly encourage other investigators to make comparative measurements of CO₂ flux in an effort to better understand and quantify the environmental controls regulating air–water gas transfer in natural settings.

References

- ALAM, A., AND J. A. CURRY. 1997. Determination of surface turbulent fluxes over leads in Arctic sea ice. *J. Geophys. Res.* **102(C2)**: 3331–3343.
- AUBLE, D. L., AND T. P. MEYERS. 1992. An open-path, fast-response infrared absorption gas analyzer for H₂O and CO₂. *Boundary-Layer Meteorol.* **59**: 243–256.
- BROECKER, W. S., J. R. LEDWELL, T. TAKAHASHI, R. WEISS, L. MERLIVAT, L. MEMERY, T.-H. PENG, B. JAHNE, AND K. O. MUNNICH. 1986. Isotopic versus micrometeorological ocean

- CO₂ fluxes: A serious conflict. *J. Geophys. Res.* **91(C9)**: 10517–10527.
- BOURASSA, M. A., D. G. VINCENT, AND W. L. WOOD. 1999. A flux parameterization including the effects of capillary waves and sea state. *J. Atmos. Sci.* **56**: 1123–1139.
- CARTER, V., N. B. RYBICKI, R. G. STRIEGL, AND P. T. GAMMON. 1997. The aquatic macrophytes in Williams and Shingobee Lakes: Implications for carbon cycling, pp. 83–88. *In* T. C. Winters [ed.], *Hydrological and biogeochemical research in the Shingobee River headwaters area, north central Minnesota*, U.S.G.S. Water Resources Investigations Report 96–4215.
- CLAYSON, C. A., C. W. FAIRALL, AND J. A. CURRY. 1996. Evaluation of turbulent fluxes at the ocean surface using surface renewal theory. *J. Geophys. Res.* **101(C12)**: 28503–28513.
- COLE, J. J., N. F. CARACO, G. W. KLING, AND T. K. KRATZ. 1994. Carbon dioxide supersaturation in the surface waters of lakes. *Science* **265**: 1568–1570.
- CRAWFORD, T. L., R. T. McMILLEN, T. P. MYERS, AND B. B. HICKS. 1993. Spatial and temporal variability of heat, water vapor, carbon dioxide, and momentum air-sea exchange in a coastal environment. *J. Geophys. Res.* **98(D7)**: 12869–12880.
- CSANADY, G. T. 1990. The role of breaking wavelets in air-sea gas transfer. *J. Geophys. Res.* **95**: 749–759.
- DANCKWERTS, P. V. 1951. Significance of liquid-film coefficients in gas absorption. *Ind. Eng. Chem.* **43**: 1460–1467.
- DEACON, E. L. 1977. Gas transfer to and across an air–water interface. *Tellus* **29**: 363–374.
- . 1981. Sea-air gas transfer: The wind speed dependence. *Boundary-Layer Meteorol.* **21**: 31–37.
- DENMEAD, O. T., AND J. R. FRENEY. 1992. Transfer coefficients for water-air exchange of ammonia, carbon dioxide and methane. *Ecol. Bull.* **42**: 31–41.
- FAIRALL, C. W., E. F. BRADLEY, J. S. GODFREY, G. A. WICK, J. B. EDSON, AND G. S. YOUNG. 1996. Cool-skin and warm-layer effects on sea surface temperature. *J. Geophys. Res.* **101(C1)**: 1295–1308.
- FAN, S.-M., S. C. WOFSY, P. S. BAKWIN, D. J. JACOB, S. M. ANDERSON, P. L. KEBABIAN, J. B. MCMANUS, C. E. KOLB, AND D. R. FITZJARRALD. 1992. Micrometeorological measurements of CH₄ and CO₂ exchange between the atmosphere and subarctic tundra. *J. Geophys. Res.* **97(D15)**: 16627–16643.
- HESSLEIN, R. H., J. W. M. RUDD, C. KELLY, P. RAMLAL AND K. A. HALLARD. 1990. Carbon dioxide pressure in surface waters of Canadian lakes, p. 413–430. *In* S. C. Wihelms and J. S. Gulliver [eds.], *Air-water mass transfer. Second international symposium on gas transfer at water surfaces*. American Society of Civil Engineers.
- HORST, T. W., AND J. C. WEIL. 1992. Footprint estimation for scalar measurements in the atmospheric surface layer. *Boundary-Layer Meteorol.* **59**: 279–296.
- JAHNE, B., K. O. MUNNICH, R. BOSINGER, A. DUTZI, W. HUBER, AND P. LIBNER. 1987. On the parameterizations influencing air-water gas exchange. *J. Geophys. Res.* **92(C2)**: 1937–1949.
- JONES, E. P., AND S. D. SMITH. 1977. A first measurement of sea-air CO₂ flux by eddy correlation. *J. Geophys. Res.* **82**: 5990–5992.
- KAIMAL, J. C., AND J. J. FINNIGAN. 1994. *Atmospheric boundary layer flows*. Oxford Univ. Press.
- , J. C. WYNGAARD, Y. IZUMI, AND O. R. COTE. 1972. Spectral characteristics of surface layer turbulence. *Q. J. R. Meteorol. Soc.* **98**: 563–589.
- KEELING, C. D., R. B. BACASTOW, A. F. CARTER, S. C. PIPER, T. P. WHORF, M. HELMANN, W. G. MOOK, AND H. ROELOFFZEN. 1989. A three-dimensional model of atmospheric transport based on observed winds: I. Analysis of observational data, p. 165–236. *In* D. H. Peterson [ed.], *Aspects of climate variability in the Pacific and the Western Americas*, Geophysical Monograph 55. American Geophysicists Union.
- KLING, G. W., G. W. KIPPHUT, AND M. C. MILLER. 1991. Arctic lakes and streams as gas conduits to the atmosphere: Implications for tundra carbon budgets. *Science* **251**: 298–301.
- KRAMM, G., R. DLUGI, AND D. H. LENSCHOW. 1995. A re-evaluation of the Webb correction using density-weighted averages. *J. Hydrol.* **166**: 283–292.
- KRAUS, E. B., AND J. A. BUSINGER. 1994. *Atmosphere-ocean interactions*. Oxford Univ. Press.
- KUDRYAVTSEV, V. N., G. L. LUCHNIK, AND A. V. SOLOVIEV. 1985. On the parameterization of the cold film on the ocean surface. *Izv. Atmos. Ocean. Phys.* **21**: 177–183.
- KWAN, J., AND P. A. TAYLOR. 1994. On gas fluxes from small lakes and ponds. *Boundary-Layer Meteorol.* **68**: 339–356.
- LABAUGH J. W., D. O. ROSENBERY, AND T. C. WINTER. 1995. Groundwater contribution to the water and chemical budgets of Williams Lake, Minnesota, 1980–1991. *Can. J. Fish. Aquat. Sci.* **52**: 754–767.
- LEUNING, R., AND J. MONCRIEFF. 1990. Eddy covariance CO₂ flux measurements using open- and closed-path CO₂ analysers: Corrections for analyser water vapour sensitivity and damping of fluctuations in air sampling tubes. *Boundary-Layer Meteorol.* **53**: 63–76.
- LISS, P. S. 1983. Gas transfer: Experiments and geochemical implications, p. 241–298. *In* P. S. Liss and W. G. N. Slinn [eds.], *Air-sea exchange of gases and particles*, NATO advanced study institute on air-sea exchange of gases and particles. D. Reidel.
- AND P. G. SLATER. 1974. Flux of gases across the air and sea interface. *Nature* **247**: 181–184.
- MACINTYRE, S., R. WANNINKHOF, AND J. P. CHANTON. 1995. Trace gas exchange across the air–water interface in freshwaters and coastal marine environments, p. 52–97. *In* P. A. Matson and R. C. Harriss [eds.], *Biogenic trace gases: Measuring emissions from soil and water*. Blackwell Science.
- MCCONNAUGHEY, T. A., J. W. LABAUGH, D. O. ROSENBERY, R. G. STRIEGL, M. M. REDDY, P. F. SCHUSTER, AND V. CARTER. 1994. Carbon budget for a groundwater fed lake: Calcification supports summer photosynthesis. *Limnol. Oceanogr.* **39(6)**: 1319–1332.
- MCMILLAN, R. T. 1988. An eddy correlation technique with extended applicability to non-simple terrain. *Boundary-Layer Meteorol.* **43**: 231–245.
- MICHMERHUIZEN, C. M., R. G. STRIEGL, AND M. E. McDONALD. 1996. Potential methane emission from north-temperate lakes following ice melt. *Limnol. Oceanogr.* **41**: 985–991.
- MOORE, C. J. 1986. Frequency response corrections for eddy correlation systems. *Boundary-Layer Meteorol.* **37**: 17–35.
- O'BRIAN, J. J. 1986. An important scientific controversy: Oceanic CO₂ fluxes. *J. Geophys. Res.* **91(C9)**: 10515.
- PENG, T. H., W. S. BROECKER, G. C. MATHEIU, Y. H. LI, AND A. E. BAINBRIGE. 1979. Radon evasion rates in the Atlantic and Pacific Oceans as determined during GEOSECS program. *J. Geophys. Res.* **84**: 2471–2486.
- PLUMMER, L. N., AND E. BUSENBERG. 1982. The solubilities of calcite, aragonite, and vaterite in CO₂-H₂O solutions between 0 and 90°C, and an evaluation of the aqueous model for the system CaCO₃-CO₂-H₂O. *Geochim. Cosmochim. Acta* **44**: 1011–1040.
- RAO, K. N., R. NARASHIMHIA, AND B. NARAYANAN. 1971. The “bursting” phenomenon in a turbulent boundary layer. *J. Fluid Mech.* **48**: 339–352.
- SCHINDLER, D. E., S. R. CARPENTER, J. J. COLE, J. F. KITCHELL, AND M. L. PACE. 1997. Influence of food web structure on carbon exchange between lakes and the atmosphere. *Science* **277**: 248–251.

- SCHUEPP, P. H., M. Y. LECLERC, J. I. MCPHERSON, AND R. L. DESJARDINS. 1990. Footprint prediction of scalar fluxes from analytical solutions of the diffusion equation. *Boundary-Layer Meteorol.* **50**: 355–373.
- SMITH, S. D., AND E. P. JONES. 1985. Evidence for wind-pumping of air-sea gas exchange based on direct measurements of CO₂ fluxes. *J. Geophys. Res.* **90**: 869–875.
- SMITH, S. V. 1985. Physical, chemical, and biological characteristics of CO₂ gas flux across the air–water interface. *Plant Cell Environ.* **8**: 387–398.
- SOLOVIEV, A. V., AND P. SCHLUSSEL. 1994. Parameterization of the cool skin of the ocean and of the air-ocean transfer on the basis of modeling surface renewal. *J. Phys. Oceanogr.* **24**: 1339–1346.
- and ———. 1996. Evolution of cool skin and direct air-sea gas transfer coefficient during daytime. *Boundary-Layer Meteorol.* **77**: 45–68.
- STURROCK, A. M., T. C. WINTER, AND D. O. ROSENBERRY. 1992. Energy budget evaporation from Williams Lake: A closed lake in north central Minnesota. *Water Resour. Res.* **28(6)**: 1605–1617.
- SUYKER, A. E., AND S. B. VERMA. 1993. Eddy correlation measurements of CO₂ flux using a closed-path sensor: Theory and field tests against an open-path sensor. *Boundary-Layer Meteorol.* **64**: 391–407.
- SZERI, A. J. 1997. Capillary waves and air-sea gas transfer. *J. Fluid Mech.* **332**: 341–358.
- TANNER, B. D., E. SWIATEK, AND J. P. GREENE. 1993. Density fluctuations and use of the krypton hygrometer in surface flux measurements. *Proceedings on Managing Irrigation and Drainage Systems*, July 21–23, Park City, Utah. American Society of Civil Engineers.
- THOMAS, F., C. PERIGAUD, L. MERLIVAT, AND J.-F. MINSTER. 1988. World-scale monthly mapping of the CO₂ ocean-atmosphere gas-transfer coefficient. *Philos. Trans. R. Soc. Lond., A* **325**: 71–83.
- VAN SCOY, K. A., K. P. MORRIS, J. E. ROBERTSON, AND A. J. WATSON. 1995. Thermal skin effect and the air-sea flux of carbon dioxide: A seasonal high-resolution estimate. *Global Biogeochemical Cycles* **9**: 253–262.
- WALLACE, D. W. R., AND C. D. WIRICK. 1992. Large sea-air gas fluxes associated with breaking waves. *Nature* **356**: 694–696.
- WEBB, E. K., G. I. PEARMAN, AND R. LEUNING. 1980. Correction of flux measurements for density effects due to heat and water vapor transfer. *Q. J. R. Meteorol. Soc.* **106**: 85–100.
- WESELY, M. L., D. R. COOK, R. L. HART, AND R. M. WILLIAMS. 1982. Air-sea exchange of CO₂ and evidence for enhanced upward fluxes. *J. Geophys. Res.* **87(C11)**: 8827–8832.
- WICK, G. A., W. J. EMERY, L. H. KANTHA, AND P. SCHLUSSEL. 1996. The behavior of the bulk-skin sea surface temperature difference under varying wind speed and heat flux. *J. Phys. Oceanogr.* **26**: 1969–1988.
- WINTER, T. C. 1997. Hydrological and biogeochemical research in the Shingobee River headwaters area of north central Minnesota (ed.), USGS Water Resources Investigations Report 96–4215.
- WOFSY, S. C., M. L. GOULDEN, J. W. MUNGER, S.-M. FAN, P. S. BAKWIN, B. C. DAUBE, S. L. BASSOW, AND F. A. BAZZAZ. 1993. Net exchange of CO₂ in a mid-latitude forest. *Science* **260**: 1314–1317.
- WOMACK, J. D., AND T. L. CRAWFORD. 1991. Description and demonstration of a continuous flow ΔpCO₂ monitor. Seventh symposium on meteorological observation and instruments, Jan. 14–18, Boston. American Meteorological Society.

Received: 13 February 1998
Accepted: 13 December 1998
Amended: 9 March 1999